

Supporting Information to:

**Blue Circularly Polarized Luminescent Molecules with Single-handed Propeller Chirality Induced by Circularly Polarized Light Irradiation**

Zhaoming Zhang,<sup>a</sup> Takunori Harada,<sup>b</sup> Adriana Pietropaolo,<sup>c</sup> Yuting Wang,<sup>a</sup> Yue Wang,<sup>a,†</sup> Xiao Hu,<sup>d</sup> Xuehan He,<sup>d</sup> Hui Chen,<sup>d</sup> Zhiyi Song,<sup>a</sup> Masayoshi Bando,<sup>a</sup> and Tamaki Nakano<sup>\*,a,e</sup>

<sup>a</sup>Institute for Catalysis (ICAT) and Graduate School of Chemical Sciences and Engineering Hokkaido University, N21W10, Kita-ku, Sapporo 001-0021, Japan

E-mail: tamaki.nakano@cat.hokudai.ac.jp

<sup>b</sup>Department of Integrated Science and Technology, Faculty of Science and Technology Oita University, Dannoharu, 700, Oita City 870-1192, Japan

<sup>c</sup>Dipartimento di Scienze della Salute, Università di Catanzaro, Viale Europa, 88100 Catanzaro, Italy, Italy

<sup>d</sup>School of Materials Science & Engineering, Nanyang Technological University, Singapore

<sup>e</sup>Integrated Research Consortium on Chemical Sciences (IRCCS), Institute for Catalysis, Hokkaido University, N21W10, Kita-ku, Sapporo 001-0021, Japan

<sup>†</sup>Present Address: Lanzhou Institute of Chemical Physics, Chinese Academy of Sciences, Tianshui Middle Road, Lanzhou, Gansu 730000, P.R. China

\*Correspondence should be addressed to Tamaki Nakano (E-mail: tamaki.nakano@cat.hokudai.ac.jp)

**Table of Contents**

Experimental details	2
Chirality switching	4
Additional CD/UV spectra	5
IR spectra	6
LD spectra	7
Changes in $g_{CD}$ of films prepared from solutions at different concentrations	8
Optimized conformations	9
Stability test	10
Aggregate structures observed through MD simulations	11
Polarized microscopic images	13
Effects of thermal annealing on chirality induction	14
AMF images	15
UV spectra in CHCl <sub>3</sub> and in CHCl <sub>3</sub> -MeOH in relation to aggregation	16
References	17

## Experimental

**Materials.** S1, S2, and S3 were available from the previous work.<sup>1</sup> Chloroform (Kanto Chemical), tetrahydrofuran (Kanto Chemical), and chloroform-d (Kato Chemical) were used as purchased. N<sub>2</sub> gas (99.99% purity) was used without drying.

**General instrumentation.** <sup>1</sup>H NMR spectra were recorded on a JEOL JNM-ECX400 spectrometer (400 MHz for <sup>1</sup>H measurement) and a JEOL JNM-ECA600 spectrometer (600 MHz for <sup>1</sup>H measurement). SEC measurements were carried out using a chromatographic system consisting of a Hitachi L-7100 chromatographic pump, a Hitachi L-7420 UV detector (254 nm), and a Hitachi L-7490 RI detector equipped with series (eluent THF, flow rate 1.0 mL/min). UV-vis absorption spectra were measured at room temperature with a JASCO V-550 and V-570 spectrophotometers. Steady-state emission spectra were taken on a JASCO FP-8500 fluorescence spectrophotometer. IR spectra were recorded on a JASCO FT/IR-6100 spectrometer using KBr pellet samples. Circular dichroism (CD) and linear dichroism (LD) spectra (Figure S4) were taken with a JASCO-820 spectrometer. The spectra were obtained by averaging those recorded at four (90° interval) or two (180° interval) different film orientations (angles) with the film face positioned vertically to the incident light beam for measurement. Linear dichroism contributions were thus minimized to afford true CD spectra. The anisotropy factor ( $g_{CD}$ ) was calculated according to  $g_{CD} = \Delta Abs / Abs = (\text{ellipticity} / 32980) / Abs$ . Differential scanning calorimetry (DSC) and thermal gravity analysis (TGA) were taken on Rigaku Thermo Plus DSC8230 and TG8120 analyzer at a heating rate of 10 K/min in nitrogen atmosphere.

**Film fabrication and CPL irradiation.** Film samples were prepared from a chloroform solution by drop-casting on to a quartz plate (1 cm x 2 cm x 0.1 cm). The film thickness was ca. 1.1 μm as measured using a Keyence VK-X3000 (interference microscope).

CPL was generated by passing light from an Ushio Optical Modulex SX-UID500MAMQQ 500-W Hg-Xe lamp through a Gran-Taylor prism and a glass-construction Fresnel Rhomb (50 mW (Jsec<sup>-1</sup>)). LPL was generated using a Gran-Taylor prism only. Irradiation experiments were conducted under N<sub>2</sub> atmosphere. Temperature regulation of film samples was performed using a tailor-made temperature controller equipped with a Peltier element-based cooler, a nichrome wire heater bridge, and a digital thermometer.

**Calculation of relative irradiation energy sum (or relative absorbed dose).** Because absorbance spectra changed as well as CD spectra on CPL irradiation, changes in  $g_{CD}$  value cannot be quantitatively discussed against simple irradiation time but should be discussed against terms of the “relative irradiation energy sum” which corresponds to the sum of

irradiation time intervals ( $\Delta t_i$ ) used to change a CD spectrum to the directly following CD spectrum multiplied by UV absorbance ( $Abs_i$ ) corresponding to the former CD spectrum according to the following equation:<sup>2,3</sup>

$$\text{Relative irradiation energy sum} = \sum_{i=0}^n \Delta t_i \times Abs_i$$

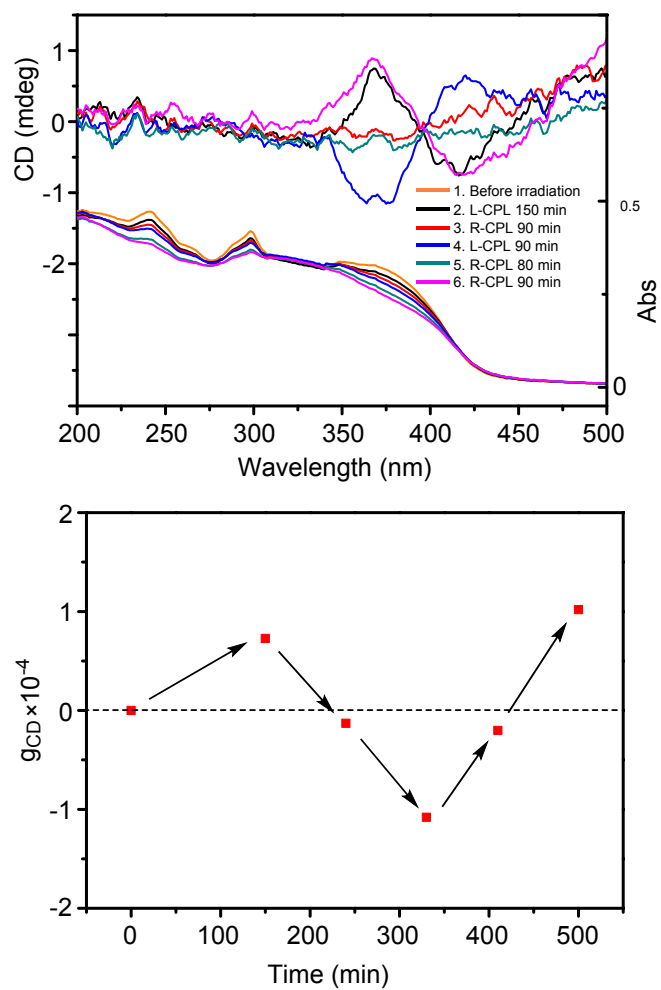
where absorbance intensity at 365 nm was considered at which the molecules mainly absorb.

**CPL emission measurements.** CPL and non-polarized fluorescence spectra were measured by using a Comprehensive Chiroptical Spectrophotometer (J-700CPL) based on the Stokes-Mueller matrix method. The excitation wavelength was set to 350 nm and the emission spectra were recorded from 700 nm to 400 nm with 860-940 V high-tension voltage, 33 mm slit width and 10 nm spectral bandwidth for the excitation and emission monochromators, respectively. For the solid-state CPL measurements, artifact-free CPL spectra were measured carefully for both enantiomeric films induced by L-CPL and R-CPL (star-shaped oligomers, S1, S2 and S3 films), employing the set of procedures based on Stokes–Mueller matrix analysis to remove parasitic artifacts, i.e., linearly polarized luminescences.<sup>4</sup>

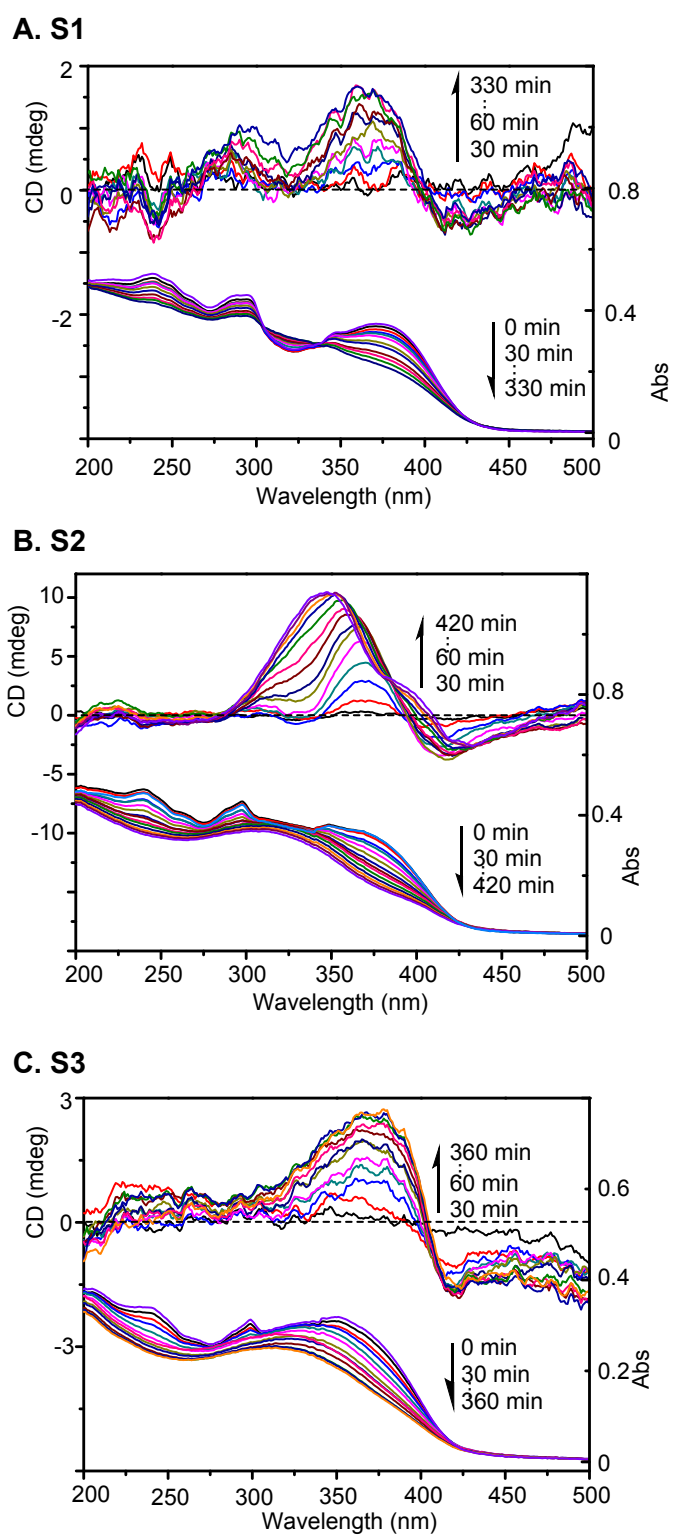
**Computational method.** Semi-empirical molecular orbital calculations by the AM1 method<sup>5</sup> were conducted using MOPAC2016 software package.<sup>6</sup> Molecular dynamic simulations in water under periodic boundary conditions were conducted using the Gromacs (ver. 5.0.7)<sup>7</sup> software with the GAFF<sup>8,9</sup> force field under a constant NPT ensemble in which the numbers of atoms, pressure, and thermodynamic temperature were held constant. Berendsen's thermocouple<sup>10</sup> was used for coupling to a thermal bath. Geometry optimization and CD/UV spectral calculations by DFT were run using Gaussian16W<sup>11</sup> package where fifty singlet excited states were estimated in the time-dependent framework using the B97D3/6-31G\* functional and the 6-31G(d) basis set.  $g_{CD}$  curve fitting were performed using Origin 2018 software package (Origin Lab)

The intrinsic rotatory strengths were calculated at the B97D3/6-31G\* level of theory<sup>12,13</sup> for all the optimized coordinates at the same level of theory, within the dipole-length formalism and reported in the usual c.g.s. units of  $10^{-40}$  esu.cm.erg/Gauss. The calculations of the ECD spectra at a given wavelength,  $\lambda$ , were done assuming Gaussian bands with  $1500 \text{ cm}^{-1}$  full width at half-height for all transitions centered at a given excitation wavelength. A factor of 2.278 was applied during the conversion of rotatory strengths and  $\Delta\epsilon$  values.<sup>14</sup> The calculations of electronic UV/VIS spectra were done in the same way, assuming the factor  $2.8710^4$  accounting for the conversion between oscillator strengths and the molar extinction coefficients.<sup>12</sup>

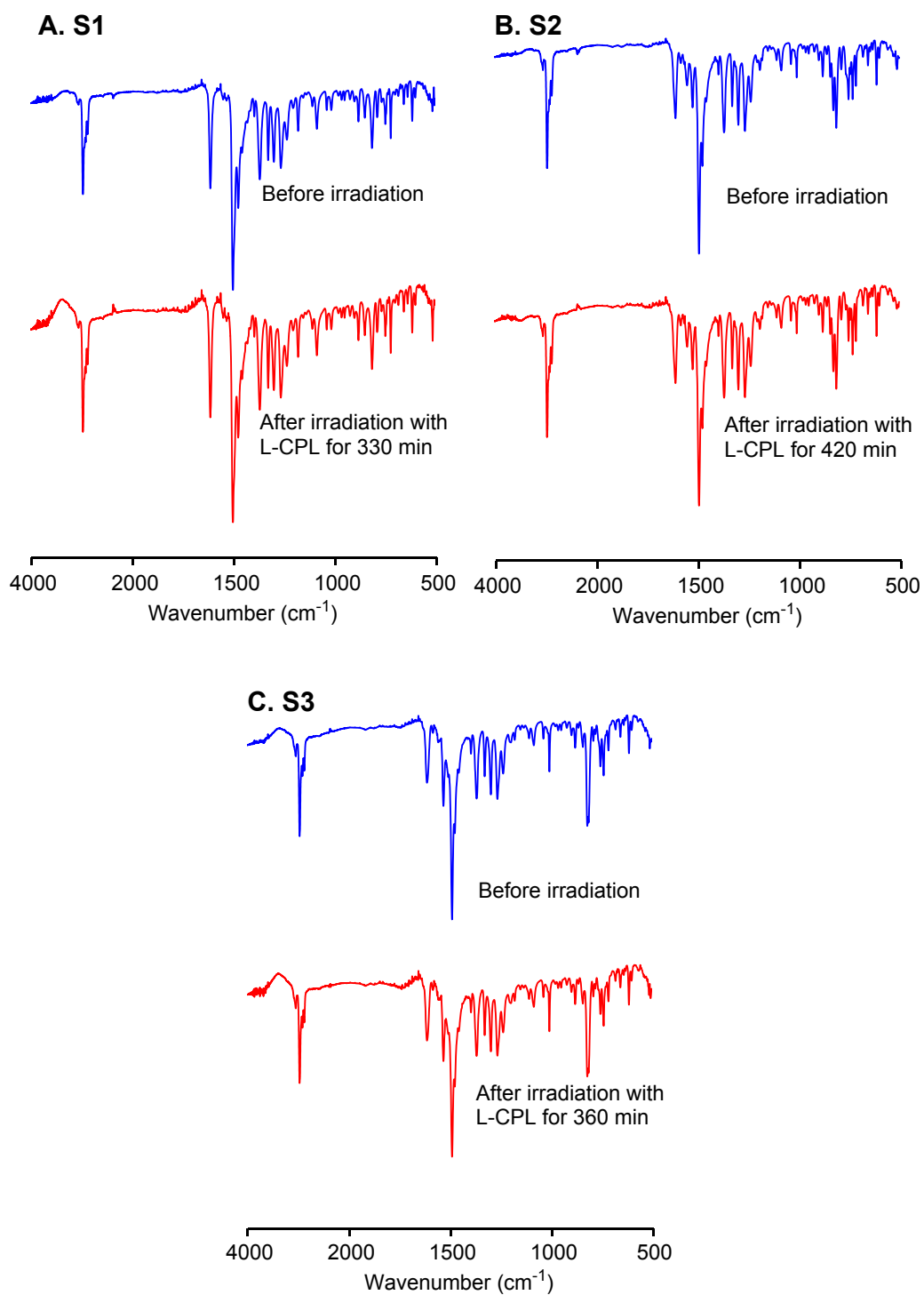




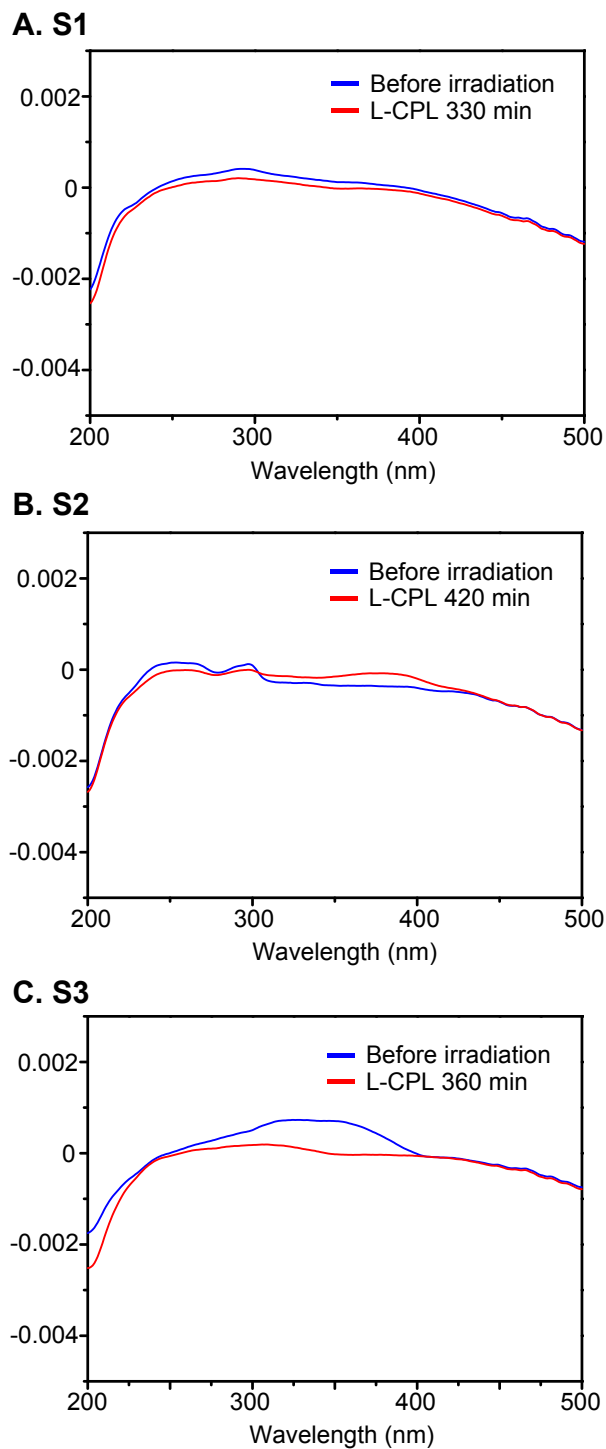
**Figure S1.** Chirality switching: changes in CD and UV spectra (A) and  $g_{CD}$  value at 368 nm (B) of S2 film on sequential irradiation with L-CPL for 150 min, with R-CPL for 90 min, with L-CPL for 90 min, with R-CPL for 80 min, and with R-CPL for 90 min to a film of S2 molecule.



**Figure S2.** Changes in CD and absorbance spectra of S1 (A), S2 (B), and S3 (C) molecules on L-CPL irradiation.

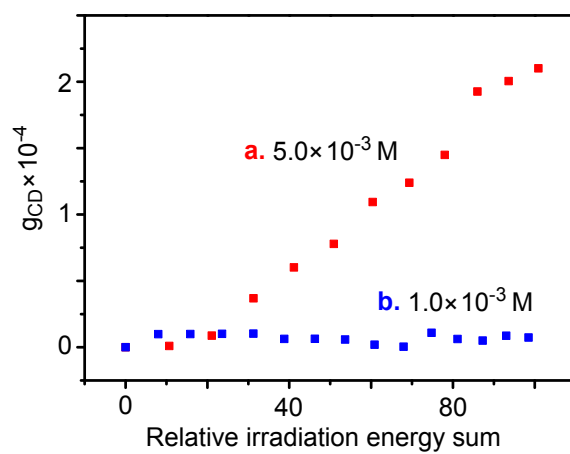
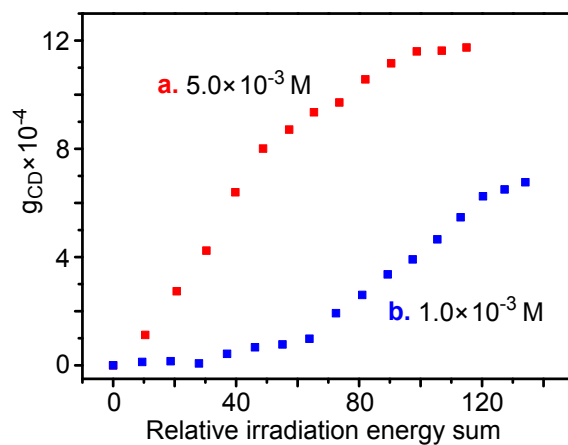
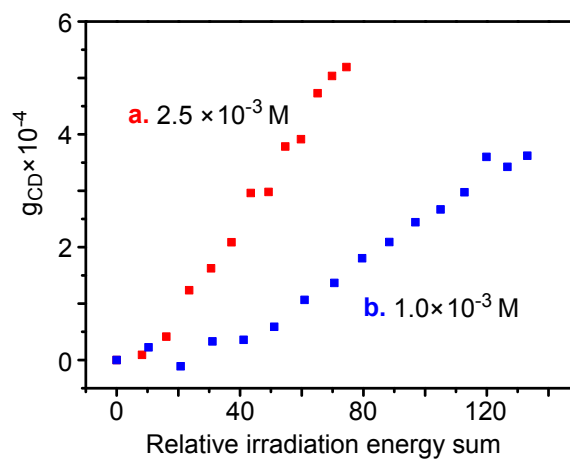


**Figure S3.** FT-IR spectra of S1 (A), S2 (B) and S3 (C) before and after CPL irradiation in film (Irradiation: 500-W Hg-Xe lamp, L-CPL, under N<sub>2</sub>). [NaCl plate]

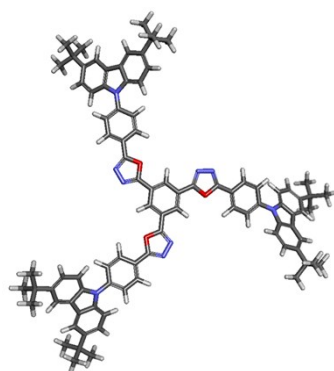


**Figure S4.** Linear dichroism (LD) spectra of S1 (A), S2 (B), and S3 (C) in film before and after CPL irradiation.

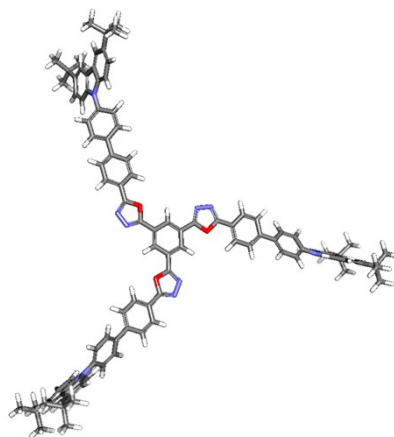


**A. S1****B. S2****C. S3**

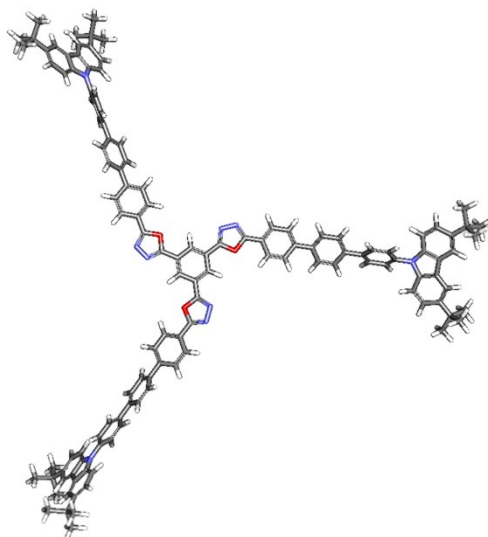
**Figure S5.**  $g_{CD}$ -vs.-relative irradiation energy sum plots of S1 (A), S2 (B), and S3 (C) in film on L-CPL irradiation. The films were prepared by solution casting from solution at different concentrations (a,b).



359.7 kcal/mol



436.3 kcal/mol



513.0 kcal/mol

**Figure S6.** Snapshots of conformations of S1, S2, and S3 having minimal total energies (AM1 method).

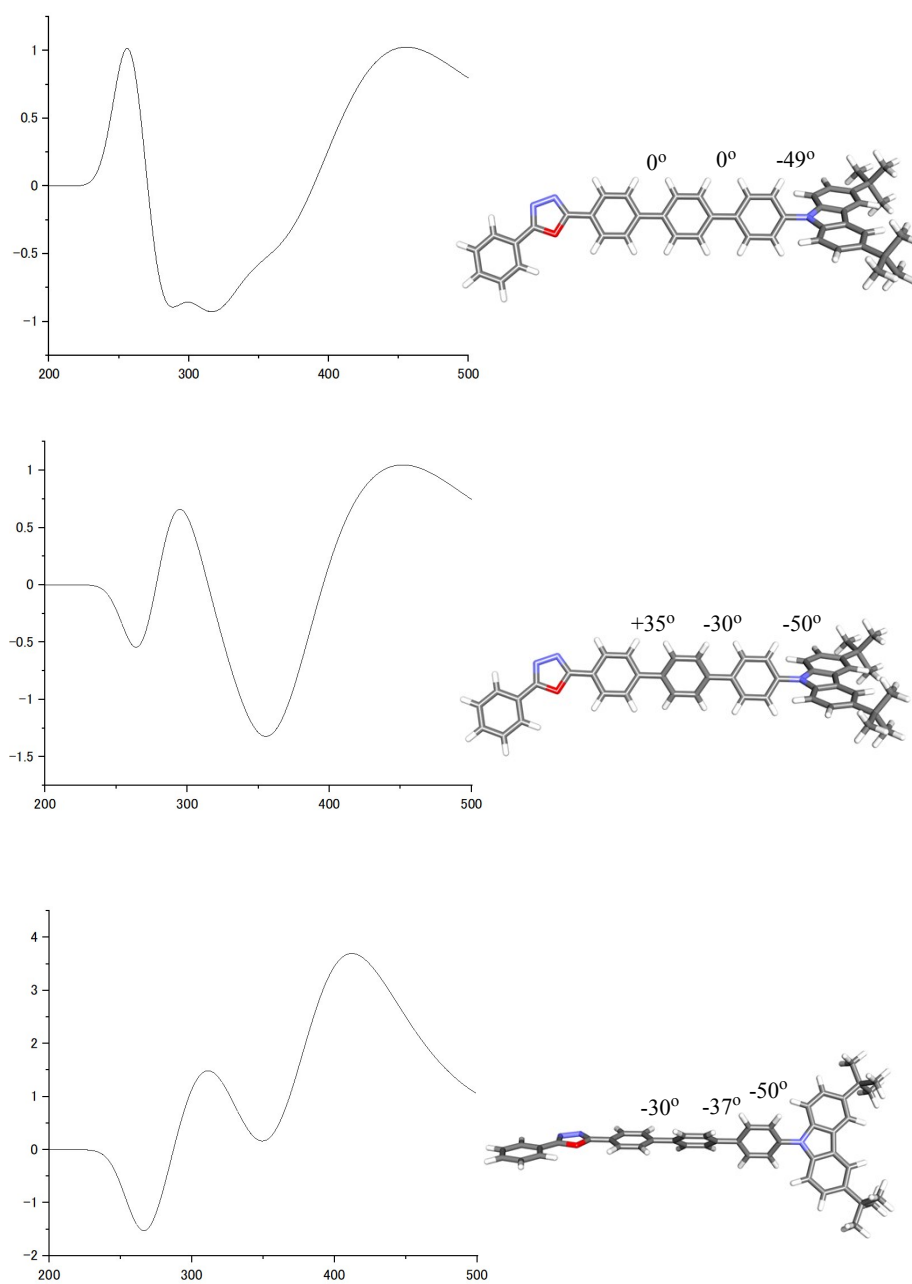


**Figure S7.** Theoretical CD spectra of S3 having different dihedral angles of the terphenyl moiety.

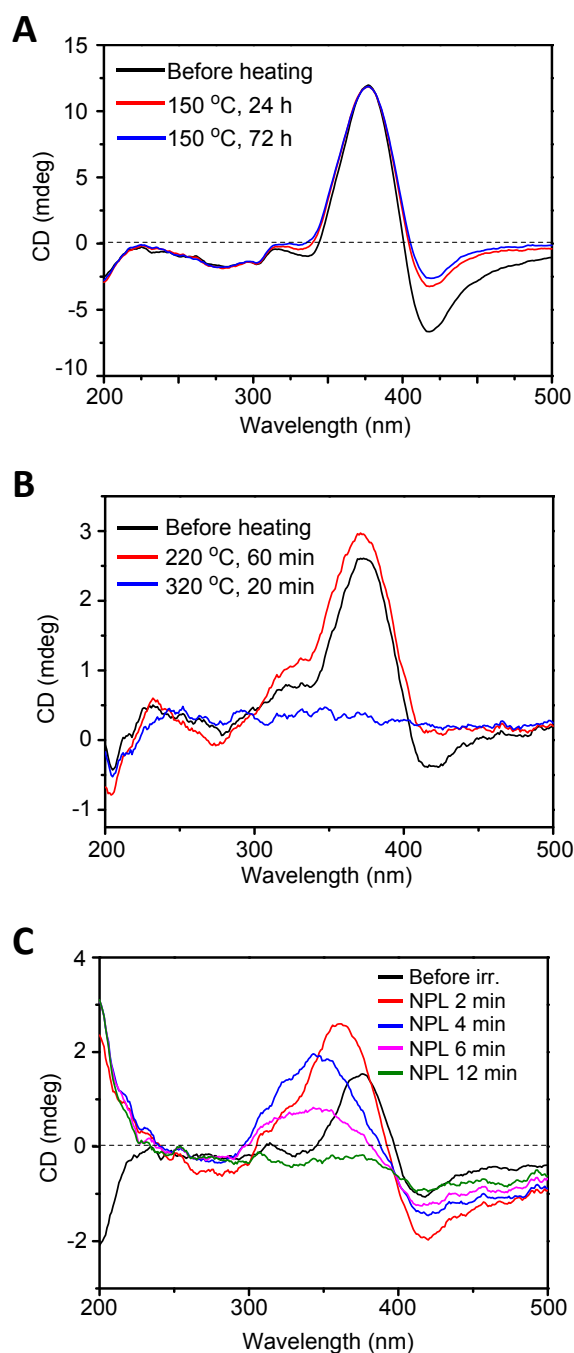


**Figure S8.** Changes in CD spectra of optically active **S2** films on heating with 150 °C for 24 h~72 h (**A**), on heating at 220°C for 60 min and on further heating at 320 °C for additional 20 min (**B**), and on irradiation with NPL for 2 min~12min (**C**). The optically active **S2** films were prepared by drop casting a solution at  $5.0 \times 10^{-3}$  M on quartz plates followed by L-CPL irradiation for 420 min.

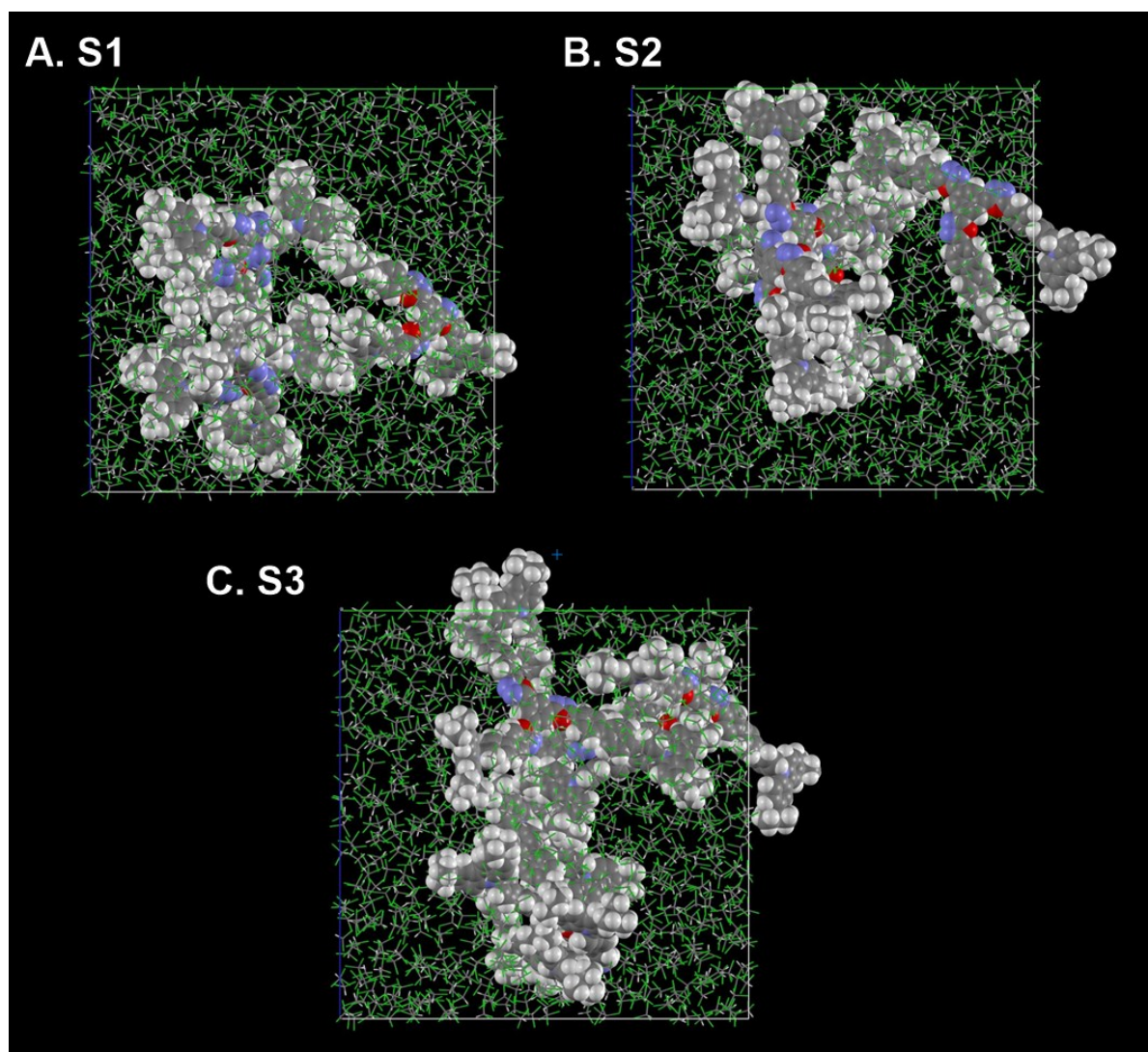
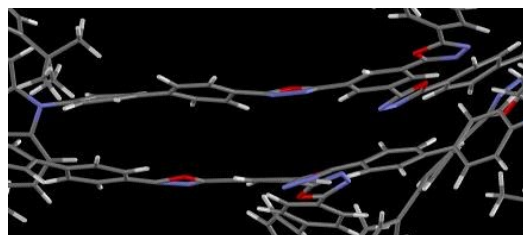
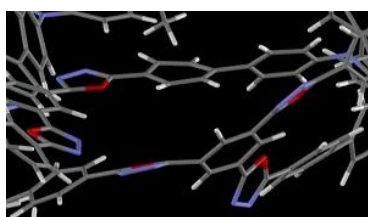


**Figure S9.** Full models of aggregate structures of five molecules of S1 (A), S2 (B), and S3 (C) observed through MD simulations in the presence of 1000 CHCl<sub>3</sub> molecules under an NPT ensemble at 300 K using periodic boundary conditions for 1 nsec. CPK models represent S1, S2, and S3, and stick models CHCl<sub>3</sub> molecules.

**S2**



**S3**

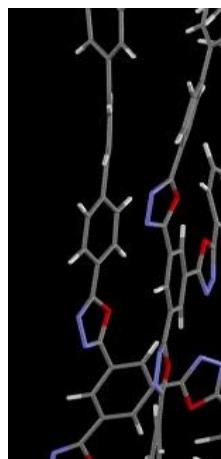
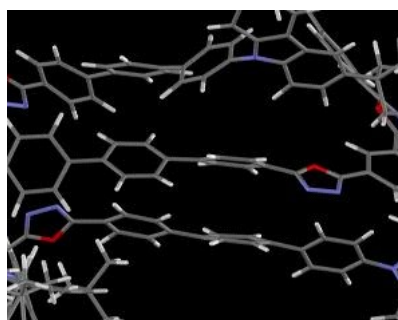


**Figure S10.** Enlarged images of  $\pi$ -stacking in the aggregates of S2 and S3 corresponding to Figure 4 B-1 and C-1 in the main manuscript.

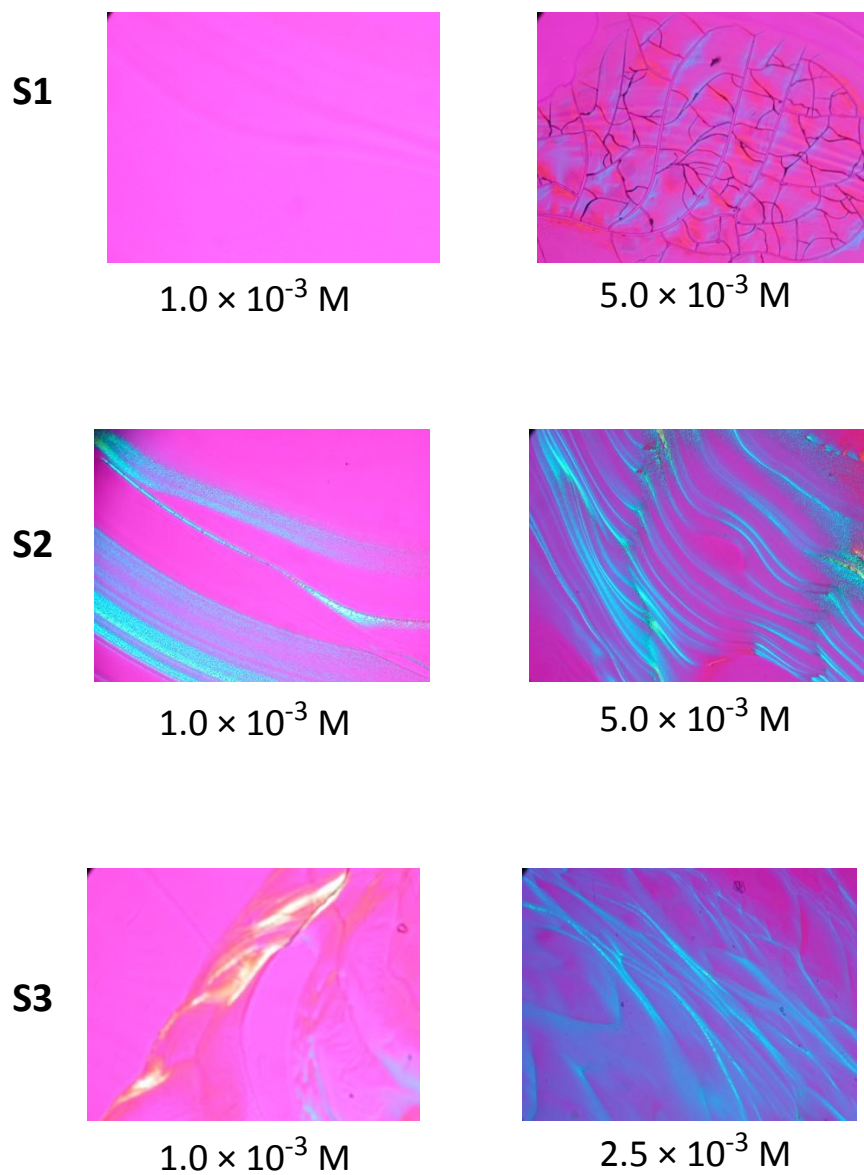


**Figure S11.** Polarized optical micrographs of films of **S1**, **S2** and **S3** prepared from different concentrations from  $\text{CHCl}_3$  solutions on a quartz plate. Concentrations of solutions used for film casting are indicated corresponding images.

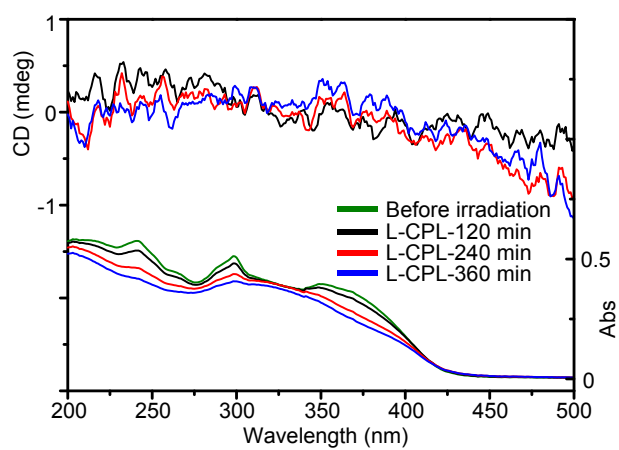
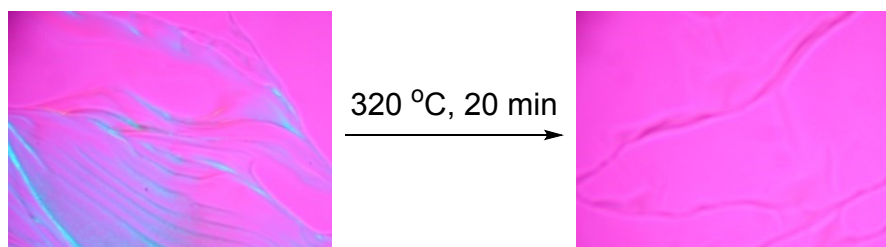


**Figure S12.** Polarized optical micrographs of an **S2** film before (A-1) and after (A-2) thermal annealing at 320 °C for 15 min, and CD/UV spectra of the annealed **S2** film observed upon irradiation of L-CPL for up to 360 min (B). The film was prepared from a solution at  $1.0 \times 10^{-3}$  M



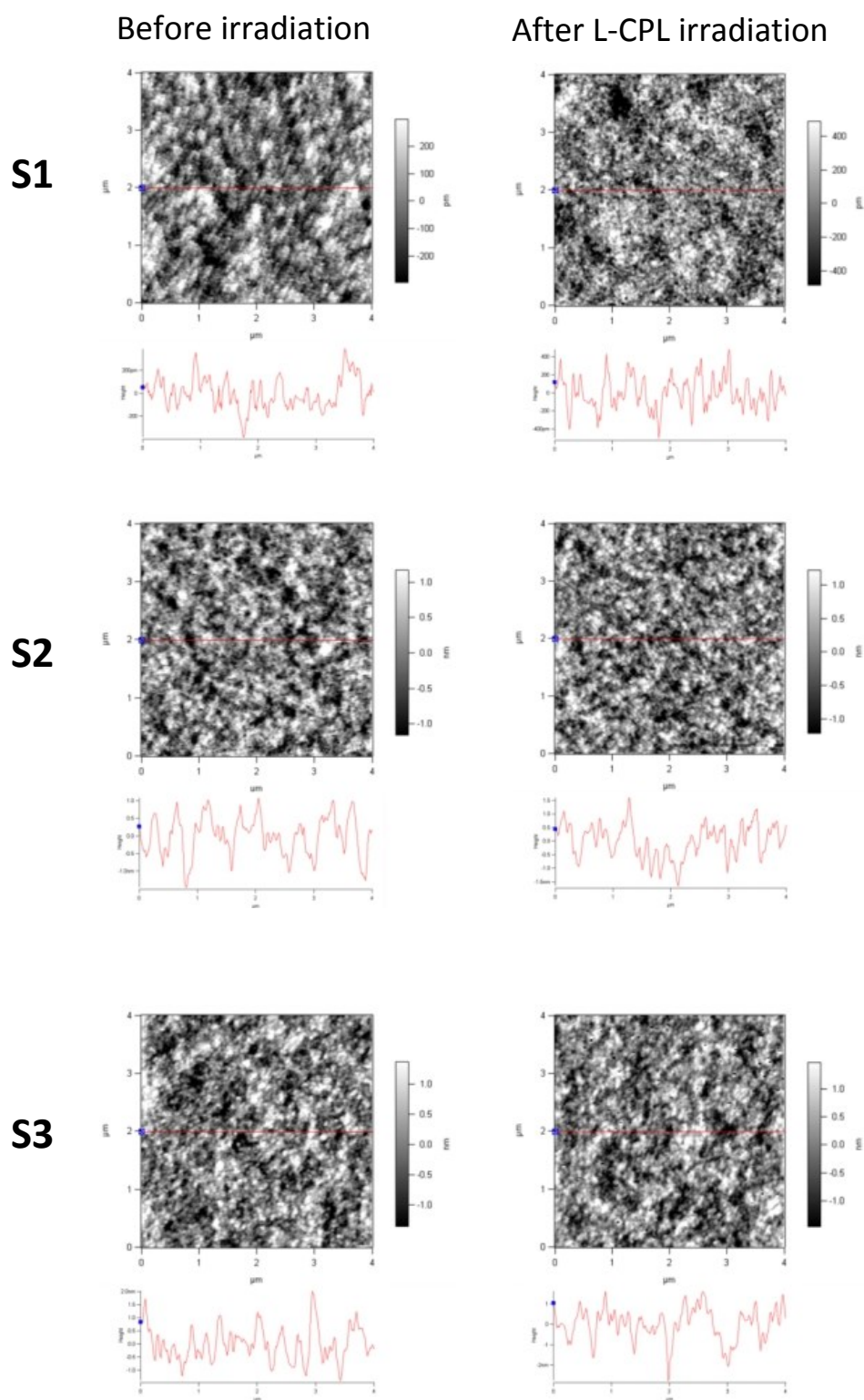


**Figure S13.** AMF images of S1, S2, and S3 deposited on HOPG surface before irradiation (left column) and after L-CPL irradiation (right column).

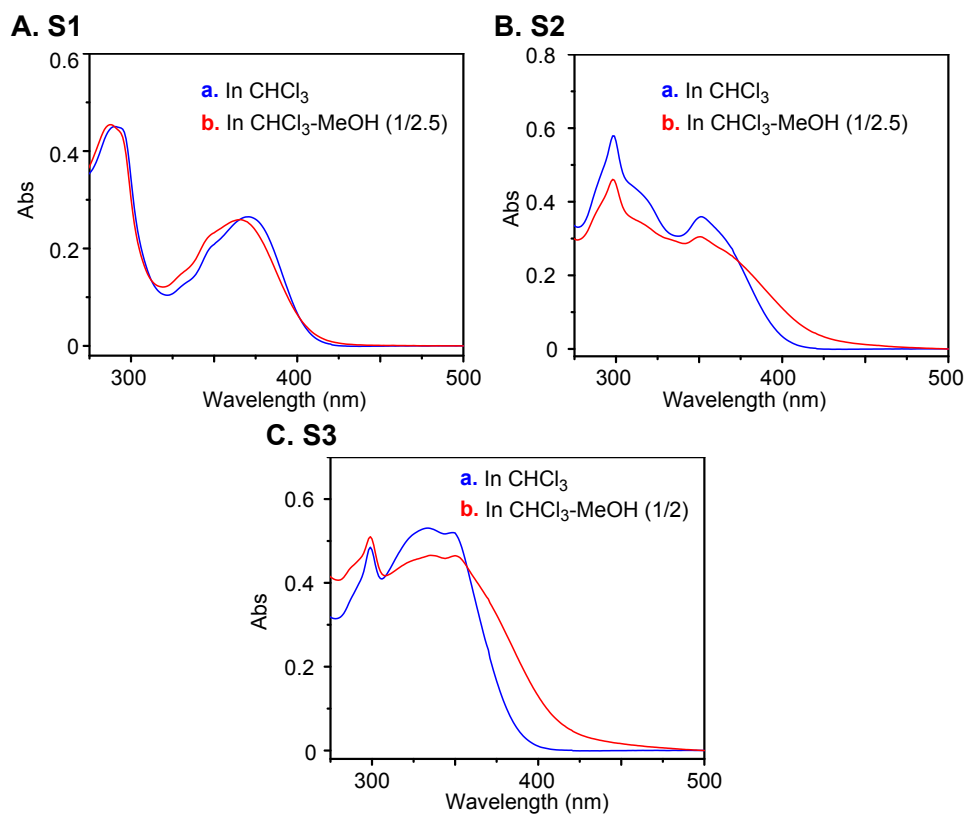


**Figure S14.** Absorbance spectra of S1 [A], S2 [B], and S3 [C] in  $\text{CHCl}_3$  (a) and in  $\text{CHCl}_3$ -MeOH (1/2.5, v/v) for A and B or in  $\text{CHCl}_3$ -MeOH (1/2, v/v) for C (b) in 1-cm cell. The spectra of A were normalized at 290 nm.

## References

1. (a) X. He, L. Chen, Y. Zhao, H. Chen, S. C. Ng, X. Wang, X. Sun, X. Hu, *Org. Electron.* **2016**, *37*, 14-23. (b) X. He, L. Chen, Y. Zhao, S. C. Ng, X. Wang, X. Sun, X. Hu, *RSC Adv.* **2015**, *5*, 15399-1540.
2. Z. Zhang, Y. Wang, T. Nakano, *Molecules* **2016**, *21*, 1541.
3. Y. Wang, T. Harada, L. Q. Phuong, Y. Kanemitsu and T. Nakano, *Macromolecules* **2018**, *51*, 6865-6877.
4. MOPAC2016, James J. P. Stewart, Stewart Computational Chemistry, Colorado Springs, CO, USA, [HTTP://OpenMOPAC.net](http://OpenMOPAC.net) (2016).
5. T. Harada, H. Hayakawa, M. Watanabe and M. Takamoto, *Rev. Sci. Instrum.* **2016**, *87*, 075102.
6. M. J. S. Dewar, E. G. Zoebisch, E. F. Healy, and J. J. P. Stewart, *J. Am. Chem. Soc.* **1985**, *107*, 3902-3909.
7. B. Hess, C. Kutzner, C. Van Der Spoel, E. Lindahl, *J. Chem. Theory Comput.* **2008**, *4*, 435-447.
8. W. Wang, P. A. Kollman, D. A. Case, *J Mol Graph Model* **2006**, *25*, 247-260.
9. J. Wang, R. M. Wolf, J. W. Caldwell, P. A. Kollman, D. A. Case, *J. Comput. Chem.* **2004**, *25*, 1157-1174.
10. H. J. Berendsen, J. V. Postma, W. F. van Gunsteren, A. R. H. J. DiNola, J. R. Haak, *J. Chem. Phys.* **1984**, *81*, 3684-3690.
11. Gaussian 16, Revision C.01, M. J. Frisch, G. W. Trucks, H. B. Schlegel, G. E. Scuseria, M. A. Robb, J. R. Cheeseman, G. Scalmani, V. Barone, G. A. Petersson, H. Nakatsuji, X. Li, M. Caricato, A. V. Marenich, J. Bloino, B. G. Janesko, R. Gomperts, B. Mennucci, H. P. Hratchian, J. V. Ortiz, A. F. Izmaylov, J. L. Sonnenberg, D. Williams-Young, F. Ding, F. Lipparini, F. Egidi, J. Goings, B. Peng, A. Petrone, T. Henderson, D. Ranasinghe, V. G. Zakrzewski, J. Gao, N. Rega, G. Zheng, W. Liang, M. Hada, M. Ehara, K. Toyota, R. Fukuda, J. Hasegawa, M. Ishida, T. Nakajima, Y. Honda, O. Kitao, H. Nakai, T. Vreven, K. Throssell, J. A. Montgomery, Jr., J. E. Peralta, F. Ogliaro, M. J. Bearpark, J. J. Heyd, E. N. Brothers, K. N. Kudin, V. N. Staroverov, T. A. Keith, R. Kobayashi, J. Normand, K. Raghavachari, A. P. Rendell, J. C. Burant, S. S. Iyengar, J. Tomasi, M. Cossi, J. M. Millam, M. Klene, C. Adamo, R. Cammi, J. W. Ochterski, R. L. Martin, K. Morokuma, O. Farkas, J. B. Foresman, and D. J. Fox, Gaussian, Inc., Wallingford CT, **2016**.
12. S. Grimme, *J. Comp. Chem.* **2006**, *27*, 1787-1799.
13. S. Grimme, S. Ehrlich, L. Goerigk, *J. Comp. Chem.* **2011**, *32*, 1456-1465.
14. N. Berova, K. Nakanishi, R.W. Woody. (Eds.). *Circular Dichroism: Principles and Applications*, 2nd ed., Wiley-VCH, New York, **2000**, 877.